Development of dosimetry using detectors of diagnostic digital radiography systems

Eiji Ariga
Graduate School of Environmental Studies, Nagoya University and Nagoya Daini Red Cross Hospital, 466-8650, Nagoya, Japan

Shigeki Ito and Shizuhiko Deji
Radioisotope Research Center, Nagoya University, 464-8602, Nagoya, Japan

Takuya Saze
Radioisotope Research Center, Tokushima University, 770-8503, Tokushima, Japan

Kunihide Nishizawa[a)]
Radioisotope Research Center, Nagoya University, 464-8602, Nagoya, Japan

(Received 25 August 2006; revised 3 November 2006; accepted for publication 6 November 2006; published 19 December 2006)

Dosimetry using an imaging plate (IP) of computed radiography (CR) systems was developed for quality control of output of the x-ray equipment. Sensitivity index, or the *S* number, of the CR systems was used for estimating exposure dose under the routine condition: exposure dose from 1.0 to 1.0×10^{2} μC kg^{-1}, tube voltages from 50 to 120 kV, and added filtration from 0 to 4.0 mm Al. The IP was calibrated by using a 6 cc ionization chamber having traceability to the National Standard Ionization Chamber. The uncertainty concerning the fading effect was suppressed less than 1.9% by reading the latent image 4 min±5 s after irradiation at the room temperature 25.9±1.0 °C. The *S* number decreased linearly on the logarithmic graph regardless of the beam quality as exposure dose increased. The relationship between the exposure dose (E) and the *S* number was fitted by the equation $E=a'\times S^{-b}$. The coefficient a' decreased when the added filtration and the tube voltage were increased. The coefficient b was 0.977±0.007 in all beam qualities. The dosimetry using the IP and the equation can estimate the exposure dose in a range from 9.0×10^{-2} to 5.0 μC kg^{-1} within an uncertainty of ±5% required by the Japanese Industry Standard. This dose range partially included the doses under routine condition. The doses between 1.0 and 1.0×10^{2} μC kg^{-1} under the routine condition can be shifted to the 5% region by using an absorber. The IP dosimetry is applicable to the quality control of the CR systems. © *2007 American Association of Physicists in Medicine*. [DOI: 10.1118/1.2402911]

Key words: imaging plate, quality control, sensitivity index, dose estimation

I. INTRODUCTION

The average annual frequency of diagnostic x-ray examinations between 1991 and 1996 came to 1477 per 1000 population in Japan, this being the highest in the world.[1] Although examinations provide great benefits, their use involves the risk of developing cancer.[2] The risk due to the examinations in Japan accounts for 3.2% of all the cancer risks, this also being highest in the world.[2] This percentage corresponds to about five times that of the UK's 0.6%.[2] Reduction of unnecessary diagnostic exposures is a national issue in Japan.

According to survey results in 2001, patient doses for similar examinations range over two orders of magnitude among medical facilities, hospitals, and clinics.[3] Optimization of the examinations is indispensable to reduce the unnecessary patient's dose compared with reference doses.[4] Quality assurance (QA) of x-ray equipment is one of the important factors for optimizing the examinations. QA is a procedure that will assure the output, image quality, alignments of equipment, and overall performance of x-ray equipment.[5] Quality control (QC) is a program designed to maintain the performance of x-ray equipment after the acceptance testing based on the QA.[6,7] The QC of the output consists of the QC of both exposure dose and beam quality.

Recently, CR systems have come into wide use, replacing screen-film systems.[1] The CR systems make digital x-ray images using an imaging plate (IP) as a detector. CR systems equipped with an exposure data recognizer (EDR) can automatically provide images whose optical densities are appropriate for diagnosis regardless of the exposure dose.[8] Thereby, CR systems considerably reduce the number of repeat films. EDR, however, prevents the radiological technologist from recognizing erroneous exposures when observing the images. Measurements are essential to detect erroneous exposure in CR systems.

The amount of photostimulated luminescence (PSL) emitted from the IP is linearly proportional to the exposure dose over four orders of magnitude.[9] Each CR manufacturer defines their individual output index as it is related to PSL intensity.[10] Fuji CR systems express their sensitivities by using an *S* number (S) that was specified to 400 when a dose of

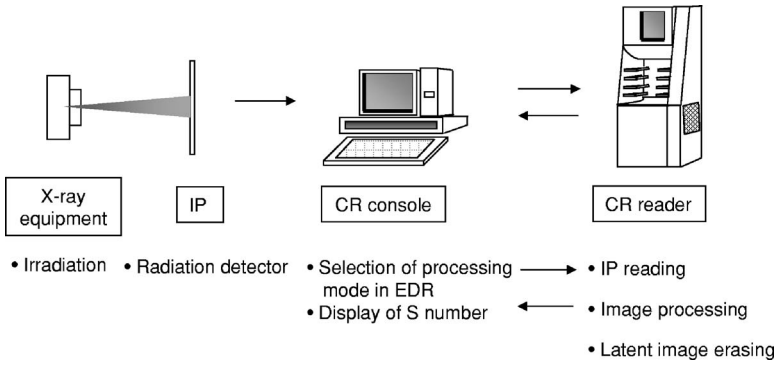

FIG. 1. Construction of the CR system.

1.29×10^{-1} μC kg^{-1} (0.5 mR) was exposed to IP at a tube voltage of 80 kV.[8] The relationship between exposure dose and the *S* number is inversely proportionate.

Several methods for estimating the exposure dose with indices relating to the PSL value have been reported.[11–15] Tatsumi *et al.*[11] reported on the dependency of the *S* number for exposure doses ranging from 0.13 to 1.3 μC kg^{-1} (0.5 to 5 mR) and the tube voltage from 40 to 120 kV. Chu *et al.*[12] showed how the *S* number decreased when the tube voltage was increased in a range between 50 and 90 kVp. These two reports did not describe the measurement uncertainty.

Shiraishi *et al.*[13] estimated the entrance surface doses of 182 patients by using the PSL value per pixel. The doses ranging from 0.8 to 25 μC kg^{-1} (from 0.03 to 0.9 mGy) were determined within an uncertainty of ±40%. Tucker *et al.* estimated two exposure doses within an uncertainty of ±5% by using the PSL value in a region of interest (ROI).[14] The two doses were 2.58×10^{-1} μC kg^{-1} (1 mR) at 60 and 80 kV, and 5.16×10^{-1} μC kg^{-1} (2 mR) at 100 and 120 kV. Floyd *et al.* estimated the entrance surface dose at two voltages of 80 and 140 kV using 1.5 mm Al with the PSL value.[15] The uncertainties were within ±12% for doses between 6 and 10 μC kg^{-1}, and within ±4% for the dose between 5.1×10^{-2} and 6 μC kg^{-1}. These authors estimated the uncertainties of the exposure doses for several specific conditions.

The examinations are routinely conducted at the tube voltages ranging from 50 to 120 kV and the added filtration ranging from 0 to 4.0 mm Al (routine condition).[16–18] According to the investigations of the entrance surface absorbed dose under routine examinations in Japan, doses ranged from 0.05 mGy for the pediatric chest to 8.6 mGy for the lateral lumbar spine.[3] These absorbed doses correspond to the exposure doses of 1.0 and 1.0×10^{2} μC kg^{-1}, respectively, when the focus-film distance is 120 cm. No reports covered the routine condition uncertainties concerning the exposure dose, the tube voltage, and the added filtration.

The exposure dose should be measured by using calibrated ionization chambers (chamber).[19,20] Japanese industrial standard (JIS) requires that the uncertainty of the chambers be less than 5%.[20] Development of a method for estimating the exposure dose with IP within an uncertainty of ±5% under the routine conditions is needed in order to apply IP to the QC of the CR system.

The purposes of this study are to analyze the dependency of an output index on exposure dose, tube voltage, added filtration; to determine the dose range meeting JIS standard; and to demonstrate the feasibility of quality control of the exposure dose with IP of the CR system.

II. MATERIALS AND METHODS

A. CR system

Figure 1 shows the constitution of a CR system. The CR system (Fuji Photo Film Co., Ltd.) is composed of x-ray equipment (DHF-155H, Hitachi Medico Co., Ltd.), an IP (ST-VN, Fuji Photo Film Co., Ltd.), a console unit (CR Console Lite, Fuji Photo Film Co., Ltd.), and a reader with EDR (FCR-5000plus, Fuji Photo Film Co., Ltd.). The x-ray equipment is comprised of an x-ray tube, an inverter-type high-voltage generator, and a collimator. The total inherent filtration consisting of the x-ray tube and the collimator was 1.8 mm in Al equivalent. The pixel size was 150×150 μm. The gray scale range was given by a 10-bit integer value.

B. Theoretical analysis

1. Relationship between exposure dose and latitude

Figure 2 shows the flow of photostimulated lights (signals) emitted from IP. Phosphor stores absorb energy in proportion to the exposure dose (E) when IP is irradiated by x rays. PSL emitted from the phosphor by a He-Ne laser beam is collected by a photomultiplier tube (PMT) through a light guide, and it is converted to a current (I). The dynamic range of the current extends over 3.6 digits.[21] The relationship between the current and the exposure dose is expressed by the following equation:[22]

$$I = d \times E, \tag{1}$$

where d is a proportional coefficient. E is expressed as follows:

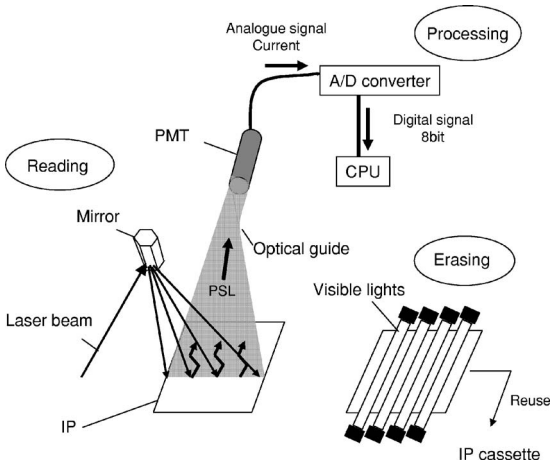

FIG. 2. Flow of photostimulated lights emitted from IP in CR reader.

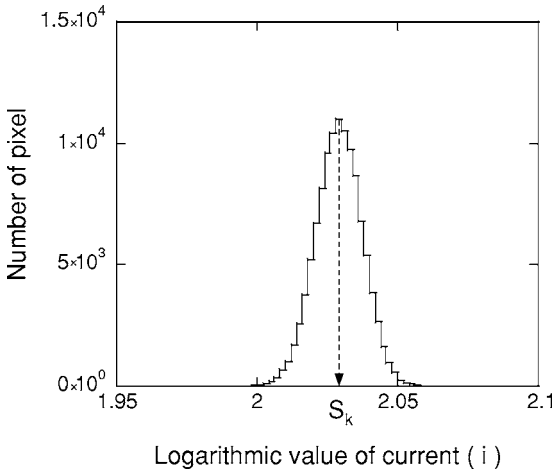

FIG. 3. Histogram of IP exposed by a flat field. The S_k of the flat field coincides with the peak of the histogram. S_k is defined to be the middle point in the range of latitude L.

$$E = \frac{1}{d}10^{i}, \tag{2}$$

where i is a logarithm of the current, $i=\log_{10} I$. The range of i was designed between 0.3 and 4.3 so that the exposure dose E corresponding to $i=2$ equals 1.29×10^{-1} μC kg^{-1} (0.5 mR) at 80 kV.[8] A default value of $d=100/0.129 = 775.2\times10^{6}$ C^{-1} kg is given in the reader.[8]

The EDR makes a distribution of the number of pixels having the same value i vs the value i (histogram). The histogram shows a pattern specific to a region of a patient's body such as head, chest, abdomen, etc. The EDR automatically selects an optimum range of the value i (latitude L) to produce images suitable for diagnosis by taking a histogram pattern into account. The middle point in the range of L was termed S_k. The S number is expressed by the following equation using S_k:[8]

$$S = 4 \times 10^{(4-S_k)}. \tag{3}$$

The EDR has four processing modes: auto, fix, manual, and semiauto. In the semiauto mode, the EDR outputs the S number calculated by using S_k equal to an average i in a ROI. The EDR was also designed so that the value L and the film density do not vary depending on the exposure. The following equation (4), obtained by substituting S_k for i in Eq. (2), expresses an average E ($\bar{E}$) per pixel in the ROI,

$$\bar{E} = \frac{1}{d}10^{S_k}. \tag{4}$$

2. Relationship between exposure dose and S number

Figure 3 shows a histogram of IP exposed by a flat field, or without objects. The S_k of the flat field coincides with the peak of the histogram. In this case, the $\bar{E}$ in Eq. (4) can be replaced by the E. Equation (5) is derived from Eqs. (3) and (4) by eliminating 10^{S_k},

$$E = \frac{a}{S}, \tag{5}$$

where the coefficient $a=4\times10^{4}\times d^{-1}$. Equation (5) was termed a general equation. The coefficient a was determined to be 51.6 by the manufacturer when IP was exposed at $E = 1.29\times10^{-1}$ μC kg^{-1} (0.5 mR) at 80 kV. The reader outputs the exposure dose E calculated using the following equation:

$$E = \frac{51.6}{S}. \tag{6}$$

Hereafter, Eq. (6) is termed a standard equation.

Equation (7) is obtained by taking logarithms of Eq. (5),

$$\log E = \log a - \log S. \tag{7}$$

This equation is a straight line with a slope of -1 on a logarithmic graph, and its intercept is $\log a$.

Equation (8) is obtained by substituting a' for a, and b for the slope -1 in Eq. (7) in order to improve the approximate precision,

$$\log E = \log a' + b \times \log S. \tag{8}$$

A linear expression of Eq. (8) is given by the following equation:

$$E = \frac{a'}{S^{b}}. \tag{9}$$

Equation (9) was termed a modified equation.

C. Measurement

1. Measurement setup

Figure 4 shows the layout of the ionization chamber and IP. The IP was calibrated by substituting IP with a 2.46 cm diameter and 3.84 cm long chamber (Radcal 9015, $10\times5-6$) which was calibrated by the National Standard Ionization Chamber.[19] Added filters were set on the lead mask

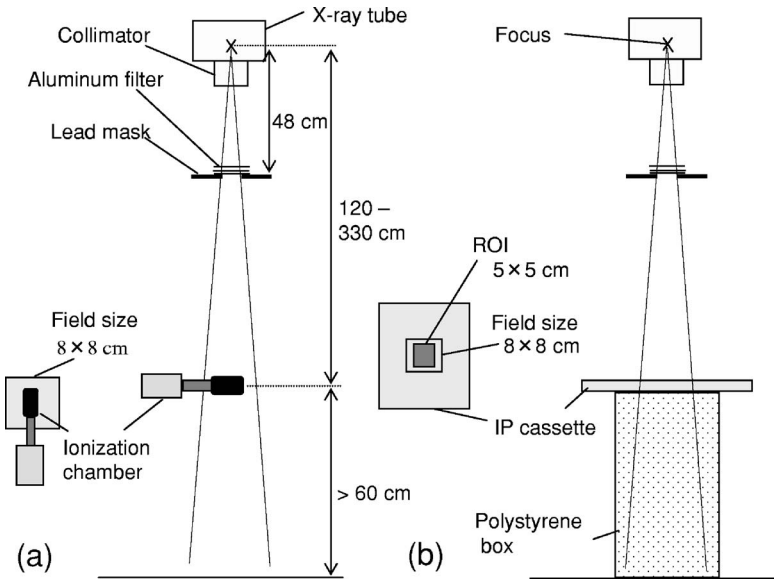

FIG. 4. Measurement arrangements of (a) ionization chamber and (b) IP.

placed at 48 cm from the focal point. The 8×8 cm exposure field contained a 5×5 cm ROI on IP and the ionization chamber. The chamber was placed 60 cm from the floor for removing the effect of backscattering. IP was irradiated at tube voltages of 50, 70, 90, and 120 kV, and the tube current was 10 mA. Three IPs were irradiated in sequence. The average S number of the three IPs was referred to the S number. Table I lists half-value layers (HVLs) for 40 combinations of 4 tube voltages and 10 added filtrations.

2. Dependency of S number on exposure dose and beam quality

The dependency of the S number on the exposure dose was evaluated at the added filtrations of 0, 2.0, and 4.0 mm Al. Exposure doses from 1.03×10^{-2} to 25 μC kg^{-1} were adjusted by controlling irradiation time from 1 ms to 8 s and FCD from 120 to 330 cm.

The dependency of the S number on the beam quality was analyzed at the added filtrations of 0, 0.3, 0.6, 1.0, 1.5, 2.0, 2.5, 3.0, 3.5, and 4.0 mm Al. Exposure doses were adjusted between 1.1×10^{-1} and 4.3×10^{-1} μC kg^{-1} by controlling irradiation time between 8 and 100 ms at FCD 120 cm.

TABLE I. Half-value layers.

Added filtration (mm Al)	Half value layer (mm Al) Tube voltage (kV)			
	50	70	90	120
0	1.58	2.04	2.53	2.94
0.3	1.70	2.22	2.76	3.27
0.6	1.82	2.39	2.98	3.57
1.0	1.96	2.60	3.25	3.94
1.5	2.13	2.85	3.56	4.35
2.0	2.28	3.07	3.84	4.72
2.5	2.41	3.28	4.11	5.06
3.0	2.54	3.47	4.35	5.37
3.5	2.66	3.65	4.58	5.65
4.0	2.76	3.82	4.80	5.92

3. Fading

The time interval from irradiation to reading (fading time) was determined by observing the fading curve[12,15] and taking into account the time required to carry the IP from the irradiation room to the reading room. IPs were irradiated for 20 ms without additional filter at 70 kV. A focus-chamber distance (FCD) was set at 100 cm. The IP was read at 1 min intervals between 2 and 10 min, at 5 min intervals between 10 and 30 min, and at 30×2^{n} min ($n=0-6$) intervals between 30 and 2200 min. Fading rates were calculated by normalizing the PSL value at any elapsed time to that at 2 min.

Temperature on the IP was measured by a thermometer with a needle-type sensor (T9631-02, HL3631, AS ONE Corp.).

4. Accuracy of IP dosimetry

The exposure doses and the S numbers were indicated as discrete numerical values on the display. An increment of adjacent numbers represents a resolution of a measurement system. The resolution of the exposure dose (E) measured by the chamber is 5.2×10^{-3} μC kg^{-1} when $E<1.04$ μC kg^{-1} and $5.0\times10^{-3}\times$E μC kg^{-1} when $E\geqslant1.04$ μC kg^{-1}. The resolution of the S number is 1 when $S<50$ and $0.03\times S$ when $S\geqslant50$. An uncertainty due to the resolution is given by $(2\sqrt{3})^{-1}$ of the increment.[23] Overall uncertainty of a dosimetry with IP (IP dosimetry) is given by a root of the sum of the square of the standard deviation of a measurement and the square of the uncertainty of the resolution.[23] The dose and the S number where the measurement uncertainty were less than 5% were termed their applicable regions.

The exposure dose measured with the ionization chamber [reference dose (D_r)] was compared with the doses (D_e) calculated by Eqs. (5), (6), and (9). Accuracy of the IP dosim-

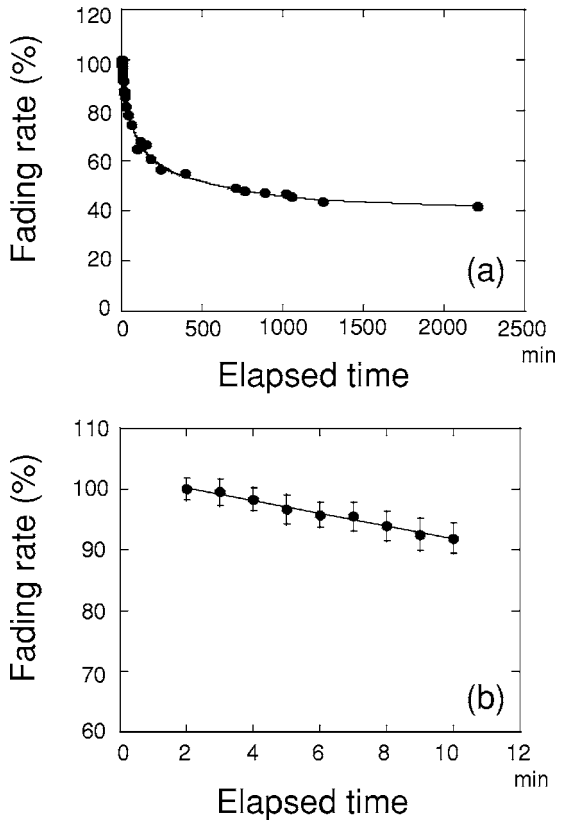

FIG. 5. Fading rate. (a) 2–2200 min, and (b) 2–10 min. Fading rates were normalized to the PSL value at 2 min. IP temperature was 25.9±1.0 °C.

etry was represented by using a relative discrepancy between the reference dose and the calculated dose, $100(D_r - D_e)D_r^{-1}\%$.

III. RESULTS

A. Fading

Figure 5(a) shows a fading curve. The IP's temperature was 25.9±1.0 °C. The PSL value decreased from 100% at 2 min to 40% at 2200 min with increasing elapsed time. Figure 5(b) shows the fading within 10 min. The relationship between the elapsed time (x) and the fading rate (y) during the first 10 min after irradiation was approximated linearly by the following equation:

$$y = -1.1x + 102. \tag{10}$$

The coefficient of correlation (R^2) was 0.988. The uncertainties of the fading rates were less than 2.7%. It took 4 min±5 s from irradiation to reading. Fading rates at 4 min and 4 min±5 s calculated with Eq. (10) were 97.6%, 97.7%, and 97.5%, respectively, and they agreed within ±0.1%. Overall uncertainties concerning fading at 4 min were less than 1.9%. Hereafter, all IPs were measured 4 min after irradiation.

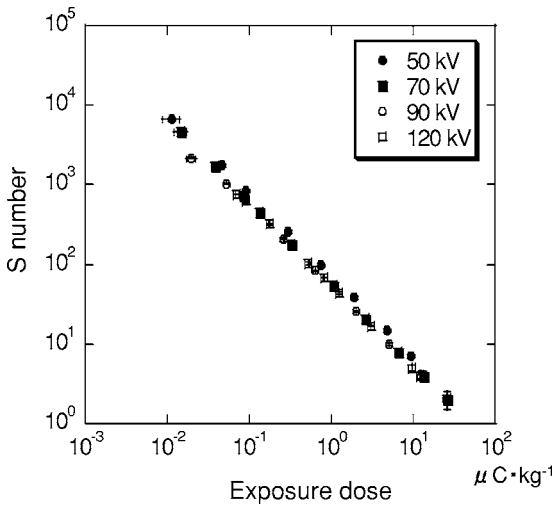

FIG. 6. Relationship between exposure dose and S number. Additional filter: 4 mm Al, and tube voltage: 50, 70, 90, and 120 kV.

B. Dependency of exposure dose on S number

Figure 6 shows the relationship between the exposure dose and the S number when the added filtration was 4 mm Al and the tube voltages were 50, 70, 90, and 120 kV. The S number decreased linearly regardless of the tube voltage as the exposure dose increased. The relationships obtained at the added filtrations of 0 and 2 mm Al showed similar tendencies.

Figure 7 represents the measurement uncertainty of the 6 cc ionization chamber for the beam qualities: tube voltage 50–120 kV, the added filtrations 0–4.0 mm Al, and the dose $1.03\times10^{-2}\sim25$ μC kg^{-1}. The uncertainty was approximated by an inverse proportional equation. The uncertainty decreased as the dose increased, and showed lower values than 5% in doses over 0.05 μC kg^{-1}. The chamber satisfied the JIS requirement for 5% uncertainty in a dose region beyond 0.05 μC kg^{-1}.

Figure 8 shows the uncertainty of the IP under the same exposure conditions as the chamber in Fig. 7. The uncer-

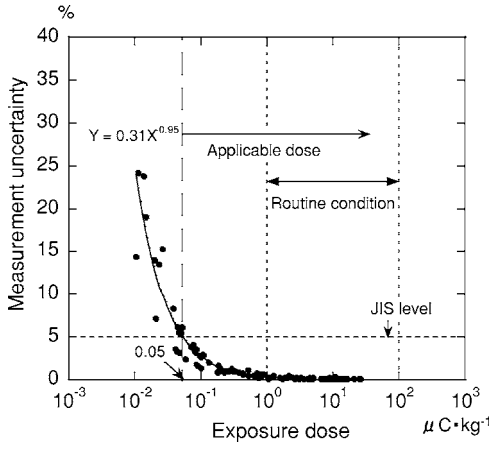

FIG. 7. Measurement uncertainty of ionization chamber. Tube voltage 50–120 kV, the filter 0–4.0 mm Al, and the dose $1.03\times10^{-2}\sim25$ μC kg^{-1}.

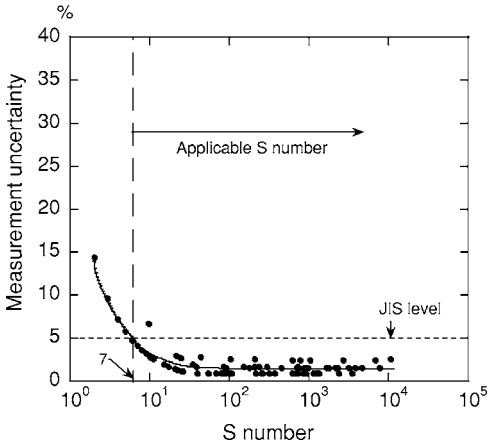

FIG. 8. Measurement uncertainty of IP.

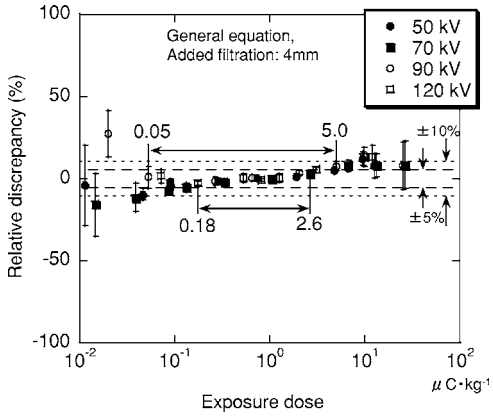

FIG. 10. Relative discrepancy between measured dose and dose calculated with general equation. Added filtration: 4 mm Al, and tube voltage: 50, 70, 90, and 120 kV.

tainty decreased as the S number increased, and showed lower values than 5% in regions between 7 and 10^4 with the exception of $S=10$. The IP dosimetry satisfied the JIS requirement for the uncertainty 5% in a region over 7.

Figure 9(a) shows the relative discrepancy between the reference dose and the calculated dose with the standard equation (6) at an added filtration of 0 mm Al. The dot and dash lines show ±5% and ±10%, respectively. The discrepancies increased as the exposure dose and tube voltage increased. The relative discrepancies at 50, 70, 90, and 120 kV ranged from −52% to −47%, from −36% to −31%, from −30% to −19%, and from −25% to −12%, respectively. The relative discrepancies were larger than 10%. Figure 9(b) shows the distribution of the relative discrepancies at an added filtration of 4 mm Al. The relative discrepancies decreased when the added filtration was increased. The relative discrepancies at 70, 90, and 120 kV were distributed partially within ±5%. The relative discrepancies at an added filtration of 2.0 mm Al showed middle values between the filtration of 0 and 4 mm Al.

Figure 10 shows the relative discrepancy between the reference dose and the calculated dose with the general equation (5) at the added filtration of 4 mm Al. The relative discrepancies were less than 5% in a dose range from 0.18 to 2.6 μC kg^{-1}. The relative discrepancies at the added filtrations of 0 and 2 mm Al showed similar dependency.

Figure 11 shows the relative discrepancy between the reference dose and the calculated dose with the modified equation (9) at the additional filter of 4 mm Al. The relative discrepancies were less than 5% in a dose range from 9.0 $\times 10^{-2}$ to 5.0 μC kg^{-1}. The region less than 5% obtained with the modified equation was 3.8 times of that obtained

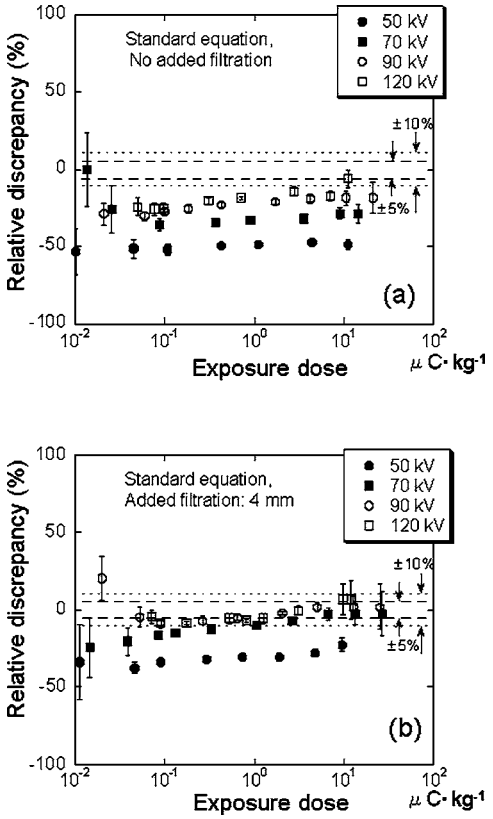

FIG. 9. Relative discrepancy between measured dose and dose calculated with standard equation. Added filtration: (a) 0 mm Al and (b) 4 mm Al, and tube voltage: 50, 70, 90, and 120 kV.

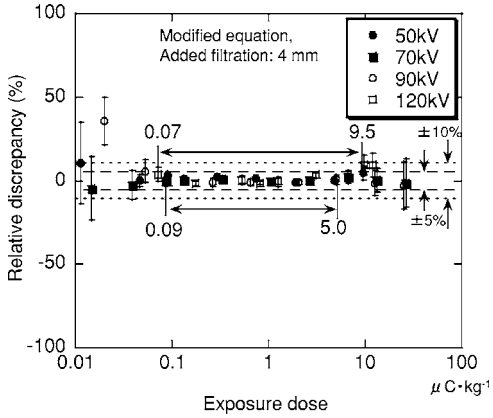

FIG. 11. Relative discrepancy between measured dose and dose calculated with modified equation. Added filtration: 4 mm Al, and tube voltage: 50, 70, 90, and 120 kV.

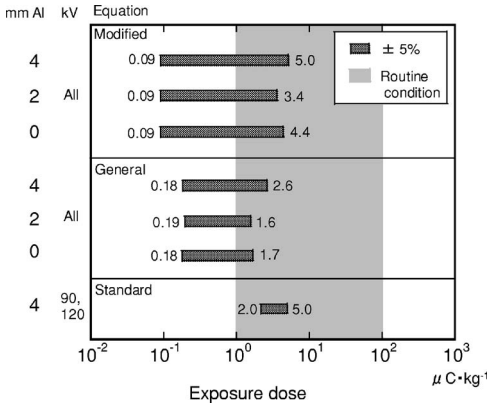

FIG. 12. Comparison of the applicable dose regions corresponding to an uncertainty less than 5% among the three equations (standard equation, general equation, and modified equation).

with the general equation. The standard deviations showed a larger value than 5% in the low doses between 0.05 and 0.09 μC kg^{-1}, and in the high doses between 5 and 20 μC kg^{-1}. Each relative discrepancy, however, was smaller than 5%.

Figure 12 compares the applicable dose regions corresponding to an uncertainty less than 5% among the three equations. The applicable dose regions of the standard equation were between 2.0 and 5.0 μC kg^{-1} only at 90 and 120 kV at 4 mm Al. The standard equation was effective under limited conditions. The applicable dose regions of the general equation were between 0.18 and 2.6 μC kg^{-1} at 4 mm Al and between 0.18 and 1.7 μC kg^{-1} at 0 and 2 mm Al. The general equation was effective for about one digit. The applicable dose region of the modified equation covered doses between 9.0×10^{-2} and 4.0 μC kg^{-1}. The modified equation was effective in 1.7 digits. The dose range of 0.7 digits out of the 1.7 digits was included in the routine.

Figure 13 shows the relationship between the added filtration and the coefficients (a) a or (b) a'. The coefficients a and a' decreased following quadratic functions when the added filtration and the tube voltages increased. The coefficients a and a' of the low voltage were larger than those of the high voltage at all filtrations with the exception of a' at 120 kV. The coefficient a' of 120 kV was approximately constant in the filtration beyond 2 mm Al. The coefficient b was distributed between 0.965 and 0.989, and the mean was 0.977. The b indicated no specific tendency.

IV. DISCUSSION

Practical reference dosimeters must have an uncertainty less than 3% in accordance with JIS. The uncertainty of measurements including variable x-ray outputs should also be less than 5%.[20] The relationships between the exposure dose and the S number, or the sensitivity index of the CR systems, were quantitatively analyzed for 160 combinations of 10 exposure doses, 4 tube voltages, and 10 added filtrations. The relationship was effectively approximated by the modified equation (9) as shown in Fig. 11. The uncertainty of less than 5% required by the JIS was attained by using Eq. (9) in the doses ranging from 0.09 to 3.4 μC kg^{-1}. The IP dosimetry met the JIS standard in this dose range. This region included the restricted dose ranging between 1.0 and 5.0 μC kg^{-1} in

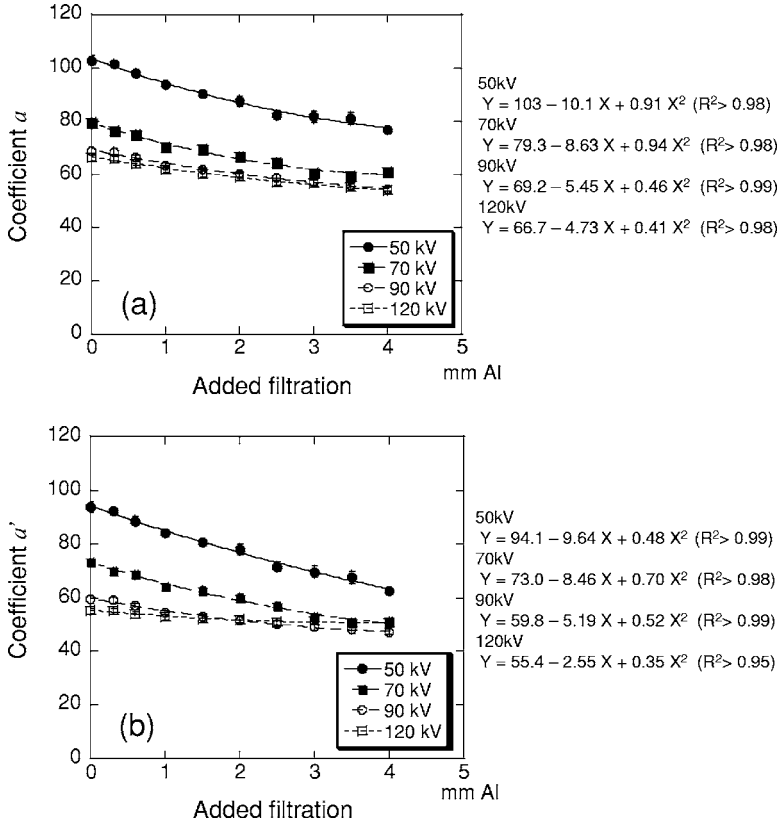

FIG. 13. Dependency of coefficients a and a' on filtration and tube voltage. (a) a is the coefficient of the general equation $E=a\times S^{-1}$, and (b) a': the coefficient of modified equation $E=a'\times S^{-b}$.

the routine. The accuracy of the IP dosimetry in this dose region was equivalent to that of the practical reference dosimeter with the traceability. Thus, IP dosimetry can be applied to quality control in a restricted dose region in the routine.

Fading affects the uncertainty of the measurements. The fading rate varied depending on the temperature and the fading time, or the time interval between irradiation and measurement. The temperature of the IP was kept constant at 25.9±1.0 °C during experimentation. Floyd *et al.* recommended reading the IP 60 min after irradiation for minimizing the fading influence.[15] Sixty min fading time is too long, because the PSL value decreases to about 70% after 60 min as shown in Fig. 5, and the background PSL increases proportional to the elapsed time. The fading and the increased background degrade image quality. The fading time should be as short and constant as possible. Thus, the fading time was kept within 4 min±5 s. When the time fluctuated within ±5 s, the fading rate calculated with Eq. (10) fluctuated less than 0.1%. Consequently, the error due to the fading effect was less than 0.1% in all measurements. The fading effect was suppressed to less than 1.9% including the measurement error. The fading effect was negligible.

The uncertainty of the 6 cc ionization chamber became larger than 5% in a dose region lower than 5.0×10^{-2} μC kg^{-1} as shown in Fig. 7. It was inferred that the large uncertainty of the relative discrepancy between the reference and calculated doses in the low-dose region shown in Figs. 9–11 was caused by the large uncertainty of the ionization chamber. High-precision ionization chambers for low-dose regions are available. Thus, large uncertainties must be reduced to less than 5% by using an ionization chamber with high precision in a low-dose region below 5.0×10^{-2} μC kg^{-1}.[24] On the other hand, the uncertainty of the IP showed larger values than 5% for the S number smaller than 7, or a high-dose region as shown in Fig. 8. The large relative discrepancy in the high-dose region was produced by the large uncertainty of the S number. The large uncertainty of the S number was caused by digital resolution of one digit in the small S number region given by the CR system's software. Improving the software's resolution is difficult. The uncertainty of the S number, however, was smaller than 5% in the S number ranging between 7 and 10^4. The S numbers 7 and 10^4 correspond to the doses 8.0 and 1.0×10^{-2} μC kg^{-1}, respectively. The IP calibrated with the two ionization chambers can estimate dose regions between 1.0×10^{-2} and 8.0 μC kg^{-1} within an uncertainty of 5% (5% region). The doses between 1.0 and 1.0×10^{2} μC kg^{-1} under the routine can be shifted to the 5% region by using an absorber. Thereby, the IP dosimetry will be able to estimate the dose under the routine within an uncertainty of 5%. The effectiveness of the IP dosimetry using the absorber, however, must be investigated experimentally.

The coefficients a' decreased when the added filtration for the four tube voltages shown in Fig. 13 was increased. The CR systems must have their inherent coefficients, and may change after installation[25] due to degradation of the laser output, optical parts, etc. The coefficients a' as well as b should be calibrated periodically using the reference dosimeter.

The quality control of the x-ray equipment involves measurement of the exposure dose and the indices concerning the beam quality such as a maximum energy, effective energy, Al half-value layer, and a quality index. The indices of the beam quality are measured with Ge semiconductor detectors, ionization chambers, and x-ray analyzers. This research proved the effectiveness of IP dosimetry for the quality control of exposure doses of the CR system. In addition, if an IP can measure the beam quality instead of the above-mentioned devices, the IP dosimetry may be applied to the QC of the output and the beam quality. The most important point is that the IP dosimetry does not require any additional instruments for the QC. IP dosimetry will greatly contribute toward diffusing the QC of CR systems. The development of a method for measuring beam quality using the IP is expected in the next step.

The accuracy and effectiveness of the IP dosimetry was demonstrated for the Fuji CR system in this research. However, other manufacturers' CR systems do not necessarily use S numbers and do not always calculate a dose index from the IP in the same manner as Fuji. The effectiveness of the IP dosimetry should be confirmed for every CR system in use.

V. CONCLUSION

A method for estimating exposure doses using IP of the CR systems within the uncertainty of ±5% was developed. The sensitivity index, S number, decreased linearly on logarithmic graph regardless of the tube voltage and the added filtration as exposure dose increased. Uncertainties of the doses estimated using the S number between 7 and 10^4 are less than 5%. The modified equation satisfies the JIS requirement for the measurement uncertainty of ±5% in a dose range from 9.0×10^{-2} to 5.0 μC kg^{-1}. This dose range partially included the doses under routine examinations. The IP dosimetry is applicable to the quality control of the exposure dose of the CR systems.

[a]Electronic mail: j45616a@nucc.cc.nagoya-u.ac.jp

[1]United Nations Scientific Committee on the Effects of Atomic Radiation, Sources and effects of ionizing radiation—UNSCEAR 2000 report to the general assembly, with scientific annexes, Volume 1: Sources, Annex D: Medical radiation exposures (United Nations, New York 2000), pp. 309–314.

[2]A. B. González and S. Darby, "Risk of cancer from diagnostic X-rays: Estimates for the UK and 14 other countries," Lancet **363**, 345–351 (2004).

[3]Y. Asada, S. Suzuki, S. Fujii, M. Kobayashi, and S. Koga, "Analysis on patient exposure of diagnostic x-ray examination; result of national investigation in 2001," Japanese Journal of Clinical Radiology **47**, 1589–1592 (2002). Summary in English.

[4]J. E. Gray, B. R. Archer, P. F. Butler, B. B. Hobbs, F. A. Metler, R. J. Pizzutiello, B. A. Schueler, K. J. Strauss, O. H. Suleiman, and M. J. Yaffe, "Reference values for diagnostic radiology: application and impact," Radiology **235**, 354–358 (2005).

[5]International Commission on Radiological Protection, ICRP Pub.34 Protection of the patient in diagnostic radiology—4 Technical and physical factors in protection of the patient, in *Annals of the ICRP*, 9(2–3) (Pergamon, Oxford, 1982), pp. 22–40.

[6]American Association of Physicists in Medicine Report No. 74, "Quality control in diagnostic radiology," (Medical Physics Publishing, Madison, WI 2002), pp. 1–19.
[7]International Electrical Commission, IEC 61223–3-1, "Evaluation and routine testing in medical imaging departments—Part 3–1: Acceptance tests—Imaging performance of X-ray equipment for radiographic and radioscopic systems," (1994). p. 17.
[8]N. Nakajima, H. Takeo, M. Ishida, and N. Nagata, "Automatic setting functions for image density and range in the FCR system," Fuji Computed Radiography Technical Review **3**, 1–23 (1993).
[9]M. Sonoda, M. Takano, J. Miyahara, and H. Kato, "Computed radiography utilizing scanning laser stimulated luminescence," Radiology **148**, 833–838 (1983).
[10]E. Samei, J. A. Seibert, C. E. Willis, M. J. Flynn, E. Mah, and K. L. Junck, "Performance evaluation of computed radiography systems," Med. Phys. **28**, 361–371 (2001).
[11]D. Tatsumi, J. Shiraishi, H. Tsushima, K. Kusumi, and A. Utsunomiya, "Relationship between incident dose on the imaging plate and *S* value associated with computed radiography (CR) systems: Quantitative evaluation using uniform exposure," (in Japanese) Japanese Journal of Radiological Technology **54**, 1273–1280 (1998). Abstract in English.
[12]R. Y. L. Chu, E. N. Christian, and B. G. Eaten, "Energy dependence of photostimulable phosphor," Radiol. Technol. **73**, 299–304 (2002).
[13]J. Shiraishi, D. Tatsumi, H. Tsushima, A. Utsunomiya, K. Kusumi, and K. Doi, "Estimation of patient dose by using a digital imaging system," (in Japanese) Japanese Journal of Radiological Technology **57**, 860–867 (2001). Abstract in English.
[14]D. M. Tucker and P. S. Rezentes, "The relationship between pixel value and beam quality in photostimulable phosphor imaging," Med. Phys. **24**, 887–893 (1997).
[15]C. E. Floyd, Jr., H. G. Chotas, J. T. Dobbins III, and C. E. Ravin, "Quantitative radiographic imaging using a photostimulable phosphor system," Med. Phys. **17**, 454–459 (1990).
[16]Food and Drug Administration, "Electronic product; Performance standard for diagnostic X-ray systems and their major components; Proposed rule," 21 CFR Part 1020 (2002), pp. 76057–76061.
[17]International Electrical Commission, IEC 601–1-3, "Medical electrical equipment—Part 1: General requirement for safety, 3. Collateral standard: General requirements for radiation protection in diagnostic X-ray," (1999), pp. 15–37.
[18]R. H. Behrman, "The impact of increased Al filtration on x-ray tube loading and image quality in diagnostic radiology," Med. Phys. **30**, 69–78 (2003).
[19]American Association of Physicists in Medicine, Report of AAPM Diagnostic X-ray Imaging Task Group No. 6, "Recommendations on performance characteristics of diagnostic exposure meters," Med. Phys. **19**, 231–241 (1992).
[20]Japanese Industrial Standard, JIS Z 4511, "Methods of calibration for exposure meters, air kerma meters, air absorbed dose meters and dose-equivalent meters" (in Japanese) (Japanese Standards Association, Tokyo 2005), pp. 7–33.
[21]J. Miyahara, K. Takahashi, Y. Amemita, N. Kamiya, and Y. Satow, "A new type of X-ray area detector ultilizing laser stimulation luminescence," Nucl. Instrum. Methods Phys. Res. A **246**, 572–578 (1986).
[22]N. Mori and T. Oikawa, "The imaging plate and its applications," Adv. Imaging Electron Phys. **121**, 294–296 (2002).
[23]International Organization for Standardization, Guide to the expression of uncertainty in measurement (ISO, Switzerland 1995), pp. 9–18, 54.
[24]http://www.radcal.com/10xseries.html
[25]T. L. Fauber, J. S. Legg, and M. Q. Quinn, "Variation in CR imaging plate readers," Radiol. Technol. **74**, 15–23 (2002).